ACS Infectious Diseases

Open Access

pubs.acs.org/journal/aidcbc

Article

C7-Substituted Quinolines as Potent Inhibitors of AdeG Efflux Pumps in *Acinetobacter baumannii*

Yiling Zhu, Charlotte K. Hind, Taha Al-Adhami, Matthew E. Wand, Melanie Clifford, J. Mark Sutton,* and Khondaker Miraz Rahman*

Cite This: *ACS Infect. Dis.* 2025, 11, 626−638

Read Online

ACCESS | Metrics & More | Article Recommendations | Supporting Information

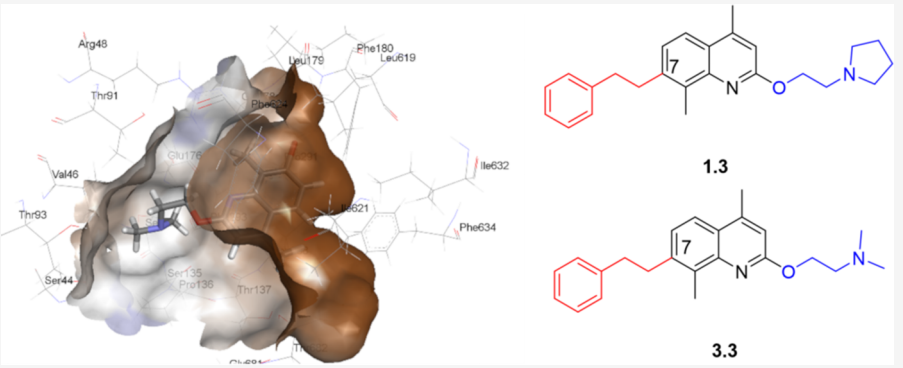

ABSTRACT: Efflux, mediated by a series of multidrug efflux pumps, is a major contributor to antibiotic resistance in Gram-negative bacteria. Efflux pump inhibitors (EPIs), which can block efflux, have the potential to be used as adjuvant therapies to resensitize bacteria to existing antibiotics. In this study, 36 quinoline-based compounds were synthesized as potential EPIs targeting resistance nodulation division (RND) family pumps in the multidrug-resistant pathogen *Acinetobacter baumannii*. In *A. baumannii* strains with overexpressed AdeFGH (chloramphenicol-adapted) and AdeABC (AYE, Ab5075-UW), these compounds enhanced Hoechst dye accumulation, indicating general efflux inhibition, and potentiated chloramphenicol, which is an AdeG substrate. The research focused on two generations of quinoline compounds, with modifications at the C-7 position of first-generation compounds to improve hydrophobic interactions with the Phe loop in the AdeG efflux pump, to generate second-generation compounds. The modified quinolines showed strong pump inhibition and significant chloramphenicol potentiation, with MIC reductions of 4- to 64-fold. Notably, compounds **1.8** and **3.8** exhibited the highest inhibitory activity, while compounds **1.3** and **3.3** showed up to 64-fold potentiation, highlighting the importance of specific structural features at the C-7 position for efflux pump inhibition. The study also revealed selective inhibition of AdeFGH over AdeABC, with no potentiation observed for gentamicin, showing the specificity of these quinoline-based inhibitors. Importantly, the compounds showed no toxicity in a *Galleria mellonella* model at a dose level of 20 mg/kg, highlighting their suitability as potential antibiotic adjuvants for combating bacterial resistance.

KEYWORDS: *Antimicrobial resistance, RND efflux pump, efflux pump inhibitors, C7-substituted quinolines, Acinetobacter baumannii*

Antimicrobial resistance (AMR) has been recognized as one of the most critical global health threats. Recently, Carbapenem-resistant *A. baumannii* has been rated by the WHO as one of the highest priority species, for which the development of new drugs is critically required.[1] *Acinetobacter baumannii* is a major nosocomial pathogen involved in epidemic infections. Like other Gram-negative bacteria, *A. baumannii* confers resistance through various mechanisms, including decreased penetration, increased efflux, overproduction of drug targets, drug target modification, enzymatic inactivation or modification of drugs, and antibiotics bypass pathway.[2] Energy-dependent efflux pumps have been suggested to contribute to a bacterium's intrinsic resistance to antibiotic activity. Among all types of efflux pumps, the resistance-nodulation-division (RND) family of efflux pumps forms a tripartite structure and spans both the inner and outer membranes of the Gram-negative bacteria. These pumps harness the proton motive force for action, and they are responsible for the efflux of a broad range of substrates.[3,4]

In *A. baumannii*, three major RND-type efflux pumps, AdeABC, AdeFGH, and AdeIJK, are each associated with the

Received: September 7, 2024
Revised: February 12, 2025
Accepted: February 18, 2025
Published: February 27, 2025

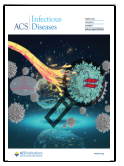

https://doi.org/10.1021/acsinfecdis.4c00705
ACS Infect. Dis. 2025, 11, 626−638

extrusion of various antibiotics. Clinically, compared to other RND efflux pumps, AdeABC is found to be overexpressed in the largest number of clinical isolates, and it contributes to the most MDR phenotype.[3] The expression of *adeABC* is positively controlled by a two-component regulatory system AdeRS.[5] Mutations in *adeRS* lead to the expression level change of AdeABC and further affect the effluxion of its substrates, including aminoglycosides, trimethoprim, chloramphenicol, fluoroquinolones, tetracyclines, *etc.*[6] AdeIJK contributes to the intrinsic resistance to β-lactams, fluoroquinolones, tetracyclines, chloramphenicol, rifampicin, and fusidic acid.[7] The expression of AdeIJK is regulated by a TetR-type regulator, AdeN and expression of an intact copy of AdeN can restore the susceptibility to antibiotics in strains with a deleted *adeN*.[8]

Compared with the other two efflux pumps in *A. baumannii*, AdeFGH appears to have the narrowest antibiotic substrate specificity, but it also contributes to MDR when overexpressed.[9] AdeL, a LysR-type transcriptional regulator, whose gene is located upstream from the *adeFGH*, is considered as a negative regulator for AdeFGH expression.[9] AdeFGH is not constitutively expressed in the wild-type strains, but it is reported as one of the most prevalent overexpressed efflux pumps in clinical strains.[3,10,11] AdeG is associated with decreased susceptibility to antibiotics, like chloramphenicol and norfloxacin.[9] Additionally, biofilm formation has also been linked with overexpressed AdeFGH, which enhances the importance of studying this efflux pump.[10] Therefore, overexpressed AdeFGH is a significant contributor to MDR in *A. baumannii*, and it is potentially an important target for developing novel antimicrobial agents and adjuvants like Efflux pump inhibitors (EPIs).

EPIs have long been considered useful adjuvants capable of restoring the activity of efflux-substrate antibiotics.[12] A number of EPIs have been identified, among them, the most well-known synthetic EPI is Phe-Arg-β-naphthylamide (PAβN), which was discovered with inhibitory activity against multiple efflux pumps including MexAB-OprM in *P. aeruginosa*, AcrAB-ToLC in *E. coli* and AdeFGH in *A. baumannii*.[13,14] Even though effects were seen from PAβN on inhibiting efflux or causing OM permeation, its further development was abandoned due to toxicity issues. Recently, specific EPIs have been described for AdeIJK. The 4,6-diaminoquoniline analogues were reported to potentiate erythromycin, tetracycline, and novobiocin in both a lab antibiotic susceptible *A. baumannii* strain and multidrug-resistant clinical isolates AB5075 and AYE.[15] So far, no stand-alone EPIs have progressed to the clinic, but this remains an attractive approach.

A quinoline-based structure (**1**) was identified by in-silico screening of a large fragment library using the homology model of the AdeB and AdeG efflux pumps in *A. baumannii* as a putative efflux pump inhibitor. Previously, compounds containing a quinoline scaffold were shown to inhibit the AcrAB-TolC pump in *Enterobacter aerogenes*.[16] This suggests that quinoline analogues can be developed as inhibitors of RND-type efflux pumps. Therefore, novel quinoline-type EPIs against *A. baumannii* were designed and evaluated by targeting the three RND-type efflux pumps, AdeABC, AdeFGH, and AdeIJK, using compound **1** as the core scaffold. Several candidates were confirmed as potential EPIs with specificity for potentiation of chloramphenicol by inhibition of AdeG. The development and evaluation of these compounds are described, and the basis for selectivity for AdeG is discussed.

RESULTS AND DISCUSSION

Antibiotic Specificity against Different RND-Type Efflux Pumps. Initially, eight antibiotics were screened against two *A. baumannii* strains (AYE and Ab5075-UW) and respective mutants in the three major RND-family efflux pumps, AdeABC, AdeFGH, and AdeIJK and their respective regulators (AdeRS, AdeL, AdeN) (Figure 1; strain information in Table S1). The antibiotics were chosen based on published efflux pump substrate specificity, such as with ciprofloxacin[17] or known potentiation by EPIs, regardless of pump identification. Only two antibiotics could be accurately ascribed as substrates for a particular efflux pump, with at least a four-fold change in MIC; gentamicin and ciprofloxacin (Table S2), which are known substrates of AdeABC in AYE.[18] All other antibiotics showed 2-fold or less change in MIC irrespective of mutation/transposons in any particular pump. This suggests that these antibiotics are not substrates for any of the efflux pumps studied, that there is redundancy among these pumps, or that expression of the pumps in these strains is at basal levels masking any effect of the mutation. Clearer results are observed in strains where the efflux pump is overexpressed, either due to a naturally occurring mutation in the regulator, as is the case for AdeABC in these strain backgrounds, or by targeted deletion/gain-of-function mutations of the repressor/activator, respectively.[19] Strains AYE and Ab5075-UW have endogenous mutations in AdeS, which lead to overexpression of AdeABC, resulting in elevated resistance to gentamicin.

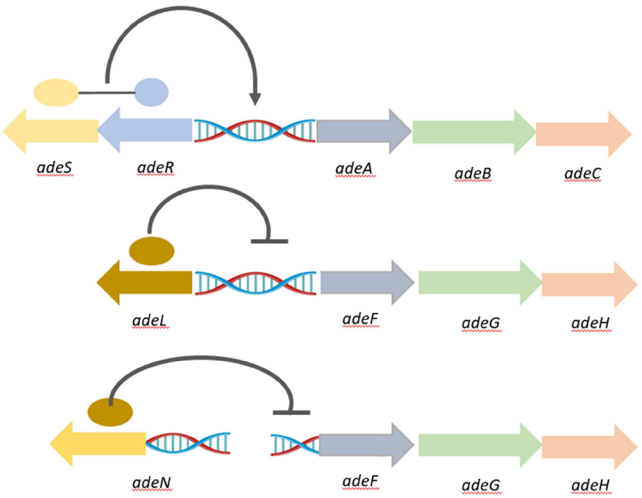

Figure 1. Schematic organization and regulation of three characterized RND efflux pump (*adeABC-RS*, *adeFGH-L*, and *adeIJK-N*) gene clusters on the *A. baumannii* chromosome.

Strains with additional overexpressed efflux pumps were generated by adapting wild-type strains to the antibiotics predicted to be substrates for a particular pump.[20] Looking to overexpress AdeFGH and AdeIJK, strains were adapted on gradient plates (Figure S1) to substrates chloramphenicol and cefotaxime, respectively.[21] Ab5075-UW was adapted to chloramphenicol exposure, generating a strain with a 4-fold increased MIC for chloramphenicol (Table S2). RT-PCR confirmed significant overexpression of AdeG (619-fold) and its regulator AdeL (four-fold) and whole genome sequencing

https://doi.org/10.1021/acsinfecdis.4c00705
ACS Infect. Dis. 2025, 11, 626−638

Scheme 1. General Reaction Scheme for Synthesis of the First-Generation Compounds[a]

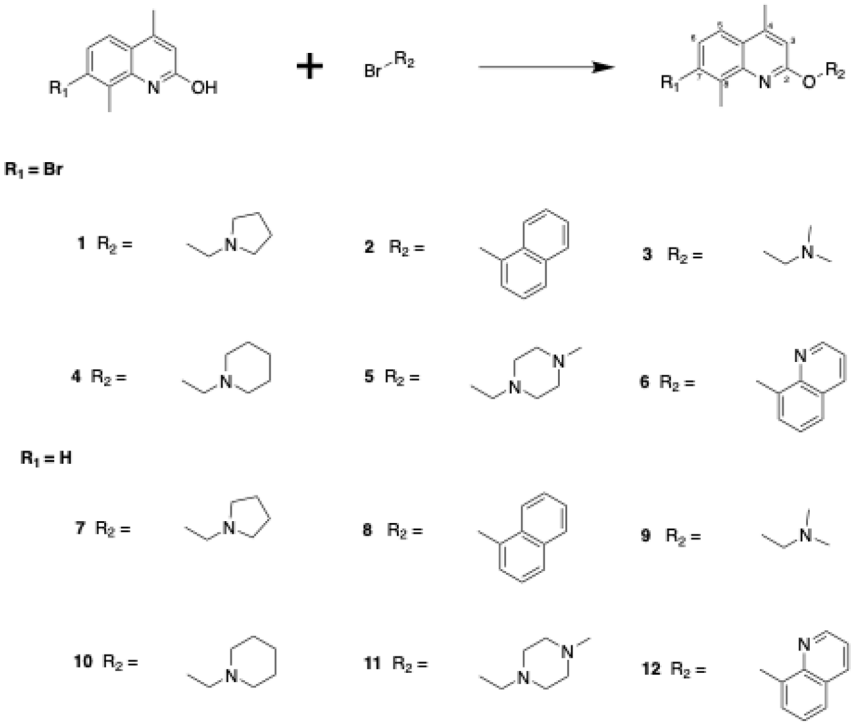

[a]To synthesize the 12 compounds, three different conditions were used. Condition 1: K_2CO_3, acetone, reflux overnight (for compounds **1**, **2**, **6**); Condition 2: K_2CO_3, DMF, reflux overnight (for compounds **3**, **7**); Condition 3; K_2CO_3, DMF, microwave 170 °C for 30 min (for compounds **4**, **5**, **8**−**12**).

confirmed an M270R mutation in the AdeFGH regulator AdeL. No significant expression level change was observed for AdeABC or AdeIJK and their regulators (Table S3). No adaptation to cefotaxime was observed for ATCC 17978, which is usually susceptible, perhaps indicating that this is a substrate for more than one pump in the strain tested.

Chemistry. Twelve first-generation quinoline-based compounds were synthesized according to Scheme 1, divided into two groups based on the presence (compounds **1**−**6**) or absence (compounds **7**−**12**) of a bromine atom at position 7 of the quinoline ring. Each group featured six different substitutions (R groups) at position C-2, including open chains, aliphatic cyclic rings, and aromatic rings designed to explore interactions with a target binding pocket.

The synthesis involved an SN2 nucleophilic substitution reaction using two starting materials: 7-bromo-4,8-dimethylquinolin-2-ol and 4,8-dimethylquinolin-2-ol. Depending on the chemical properties of the starting material, three different reaction conditions were employed. Condition 1 (overnight reflux in acetone) successfully synthesized compounds **1**, **2**, and **6** with yields ranging from 36 to 78%. Condition 2 (overnight reflux in DMF) was used when Condition 1 failed, yielding 48% and 19% for compounds **3** and **7**, respectively. Condition 3 (microwave heating in DMF) was applied when previous conditions were unsuccessful, producing the remaining compounds with yields between 14 and 44%.

The first-generation compounds were modeled against both AdeB and AdeG transporter proteins to understand the basis of the observed selectivity. Since the crystal structures of AdeB and AdeG are not available, the molecular models were developed using a homology modeling approach with the Swiss Model Web server using published crystal structures of AcrB (1IWG) and MexB (3W9J) as templates. The poses with the best ChemScore and ΔG values for compounds **1** and **3** against both efflux pump transporters are shown (Table S4). Notably, there are high-affinity interactions between both compounds and two Phe (Phe293 and Phe624) residues within the binding pocket of AdeG but only one in AdeB (Phe612) (Figure S2). This could suggest that multiple Phe residues in AdeG are important in determining inhibition and this is consistent with the known importance of a Phe loop in several efflux transporters, including AdeB.[22] Monitoring the location and orientation of the compounds in diverse complexes showed that both compounds are completely trapped in the distal pocket of the multi-binding site of AdeG whereas they are only partially trapped in the case of AdeB. Hence, the compounds are likely to form much more stable pump-inhibitor complexes in AdeG, than in the binding site of AdeB. To investigate this further, we performed structural optimization of the docked complexes, allowing flexibility for residues surrounding the ligand. This refinement resulted in negligible ligand movement within the binding site, and the ligand remained within the hydrophobic region of the distal binding pocket, particularly interacting with the Phe loop of the AdeG efflux pump (Figure S3), reinforcing our observation. At the C-7 site, the Br group of the compound was located in the hydrophobic part of the distal binding pocket of the efflux pump. Based on this, the C-7 site was selected for the introduction of further hydrophobic side chains that might interact with the hydrophobic pockets more efficiently than those in compounds **1** or **3**, with the aim of developing more potent efflux pump inhibitors. We selected a diverse range of hydrophobic C-7 side chains, including a phenyl ring, 5- and 6-membered heterocycles, benzofused

https://doi.org/10.1021/acsinfecdis.4c00705
ACS Infect. Dis. 2025, 11, 626−638

Scheme 2. Synthesis of the Compounds with C-4 and C-8 Methyl Groups (1.1−1.9, 3.1−3.9); Conditions: Pd(PPh3)4 (10% mol of 1/3), Toluene/MeOH (4:1), Reflux for 6 h/Overnight

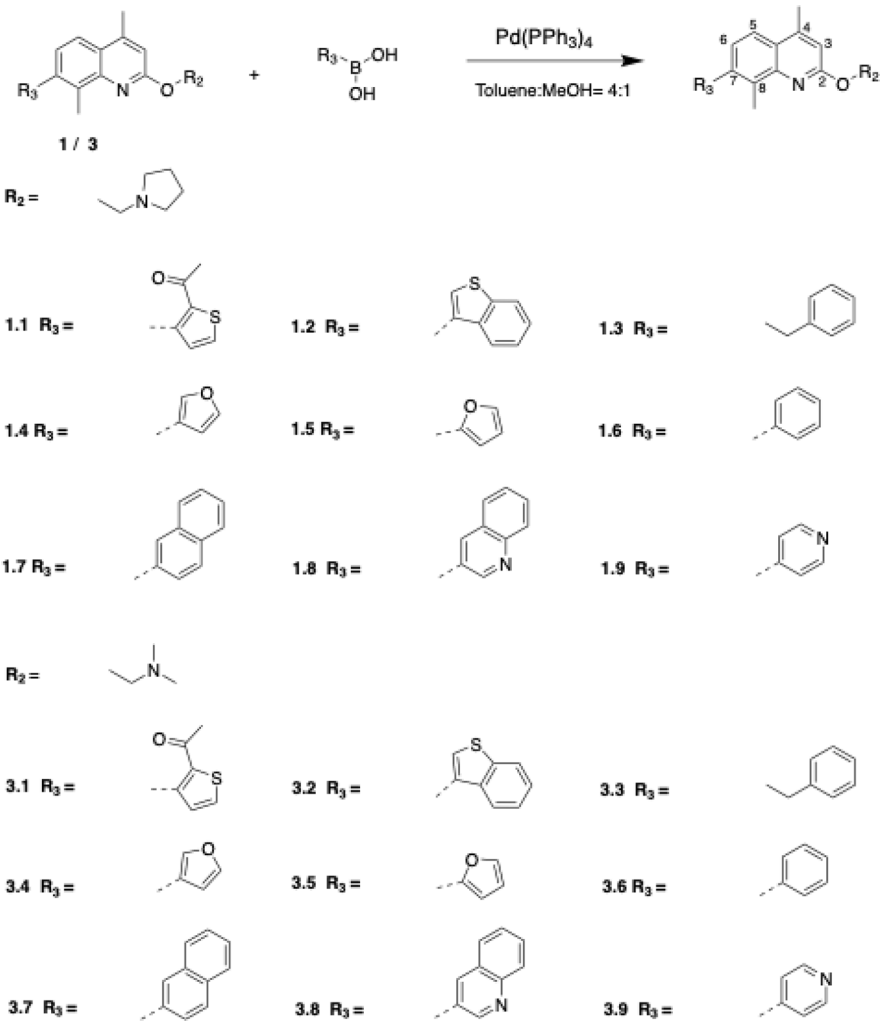

heterocycles, a second quinoline ring, a naphthalene ring, and a flexible side chain with a terminal phenyl ring.

A second generation of compounds was designed based on the best-performing first-generation compounds, **1** and **3.** Twenty-four second-generation quinoline-based compounds, designed to increase the interaction with the hydrophobic Phe loop of AdeG, were synthesized using solution phase chemistry (Schemes 2 and 3). Among these, 18 compounds featured two methyl groups at positions C-4 and C-8 of the quinoline ring, while six compounds lacked these methyl groups. The 18 compounds containing C-4 and C-8 methyl groups were derived from the first-generation compounds **1** (**1.1−1.9**) and **3** (**3.1−3.9**) through a Suzuki coupling reaction (Scheme 2). This reaction involved the use of a boronic acid, an organohalide, and a palladium (0) complex catalyst, specifically Tetrakis (triphenylphosphine) palladium (0) (Pd(PPh3)4) (Scheme 2). The boronic acids used as starting materials were commercially obtained, and the reaction was carried out in a mixture of toluene and methanol under reflux for 6 h or overnight.

The reaction conditions were consistent across the 18 compounds, where the quinoline starting material was reacted with the boronic acid in a 1:1.2 molar ratio using 100 mg of the quinoline compound (Scheme 2). The reaction progress was monitored using thin-layer chromatography (TLC) and liquid chromatography−mass spectrometry (LC−MS). Postreaction, the products were extracted, dried, and purified via flash column chromatography using a dichloromethane/methanol solvent system.

Additionally, six compounds lacking C-4 and C-8 methyl groups (**1.10−1.12** and **3.10−3.12**) were synthesized using a two-step process: initial reaction in DMF with K_2CO_3 under microwave conditions, followed by Suzuki coupling (Scheme 3). All synthesized compounds were characterized using 1H-NMR, 13C-NMR, LC-MS, and HR-MS, with purity confirmed by LC-MS analysis.

Efflux Inhibitory Activity of First-Generation Quinoline-Type EPI Compounds. Direct antimicrobial activities of the quinoline derivatives were measured on *A. baumannii* AYE and Ab5075-UW strains using MIC tests and growth curve assays. Testing concentrations (Table S5) were identified that had no significant impact on bacterial growth (defined as less than a 10% reduction in OD_{600} measured after 20h growth) compared to the wild type. Two known EPIs, PAβN and CCCP, were also tested in parallel with the quinoline series using the Hoechst assay.[23] Increased accumulation of the fluorescent dye inside the bacterial cells correlates with reduced efflux activity via one of a number of pumps through

https://doi.org/10.1021/acsinfecdis.4c00705
ACS Infect. Dis. 2025, 11, 626−638

Scheme 3. Synthesis of Compound without C-4 and C-8 Methyl Groups (1.10−1.12, 3.10−3.12); Reagents and Conditions: (I) DMF, K2CO3, Microwave (60 min). (ii) Pd(PPh3)4 (10% mol of 1.10/3.10), Toluene: MeOH = 4:1 (5 mL), Reflux Overnight

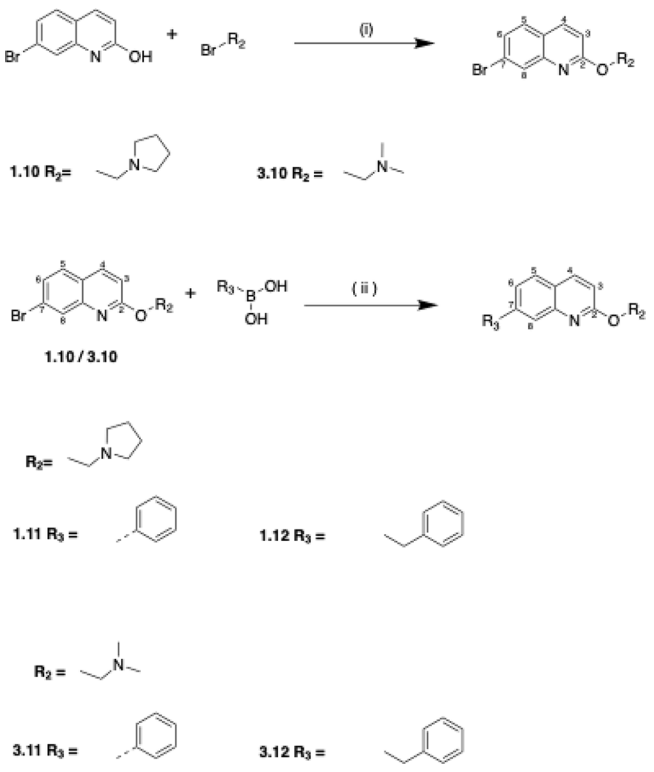

inhibition by the EPIs. AYE and AB5075-UW showed essentially identical accumulations of Hoechst over time, ensuring that studies with efflux pump/regulator mutants in either of these backgrounds are directly relatable to the Hoechst data.

Several of the quinoline compounds induced a rapid increase in fluorescence due to Hoechst accumulation and reached a steady state consistent with activity as EPIs (Figure 2). Compound **12**, containing a quinoline side chain, showed a very different profile of Hoechst accumulation, with the final fluorescence being one of the highest values measured by the end of the incubation. This possibly suggests a very different mechanism of action contributing to a reduction in efflux or inherent fluorescence of the compound due to the presence of the quinoline ring. The efflux inhibitory activity of each compound was calculated by normalizing the data at 24 min to the fluorescence level of the compound-free (control) cells (Table 1). Four of the compounds tested, compounds **1**, **3**, **4**, and **9** showed significantly higher fluorescence accumulation than the control and the others. Generally, for the pair of compounds with the same R_2 substitution, the one with Br on C-7 accumulated a higher fluorescence in the cells than the other one without Br. Among the four compounds with the best EPI activity, compound 9 is the only one that does not have a C-7 Br substitution, while its corresponding compound with C-7 Br, compound **3**, also showed significant inhibitory activity. These results suggest that the C-7 Br substitution is important for inhibitory activity. This observation led us to select compounds **1**, **3**, and **4**, all of which contain the C-7 Br substitution, for further optimization. Interestingly, the three compounds had a basic R2 side chain with a tertiary N either part of a heteroaliphatic ring (compounds **1** and **4**) or as a dimethyl amine terminal group. Compounds containing naphthalene (compounds **2** and **8**) or quinoline terminal rings (compounds **6** and **12**) did not show significant efflux inhibitory activity despite having more hydrophobic side chains.

To investigate whether the EPI candidate compounds targeted AdeABC or AdeFGH, the degree of MIC potentiation was tested with chloramphenicol and gentamicin with compounds **1**, **3**, and **4** (Table S6). None of the compounds reduced the MIC of gentamicin in the wildtype strain, and only compound **3** showed a 2−4-fold potentiation of chloramphenicol in the wildtype strain AYE. In the AdeG-overexpressing strain Ab5075-CHL, compounds **1** and **3** potentiated chloramphenicol by 4- and 8-fold, respectively. No gentamicin potentiation was observed for either PAβN or CCCP, consistent with previous data showing that neither are effective

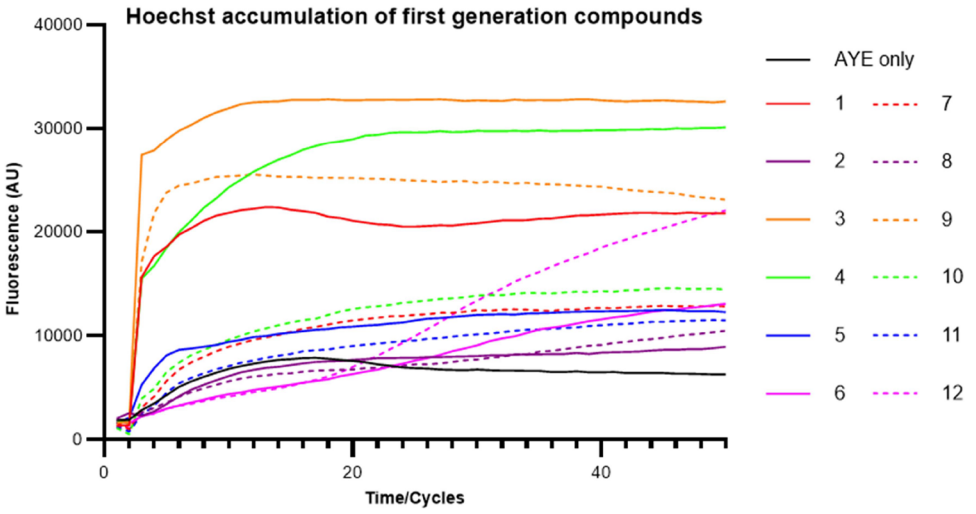

Figure 2. Hoechst accumulation in AYE cells with the addition of synthesized EPI compounds. All results were performed in triplicates and the curve presented is the fluorescence value of three biological repeats after being blanked against cell free PBSM+G with HOECHST DYE; for clarity, error bars are not shown on the graph, but the SD is included in the end-point measurements shown in Table 1.

https://doi.org/10.1021/acsinfecdis.4c00705
ACS Infect. Dis. 2025, 11, 626−638

Table 1. Inhibitory Activity of the First-Generation Compounds against Strain AYE Assessed by Changes in Hoechst Accumulation Compared to Known EPIs[a]

compound ID	inhibitory activity	*P* value*	name	inhibitory activity	*P* value
1	3.12 ± 0.11	8.5×10^{-04}	**7**	1.31 ± 0.32	0.26
2	0.91 ± 0.13	0.59	**8**	0.83 ± 0.14	0.27
3	4.57 ± 0.11	7.83×10^{-06}	**9**	3.59 ± 0.28	5.0×10^{-04}
4	3.53 ± 0.19	8.11×10^{-05}	**10**	1.41 ± 0.22	0.07
5	1.36 ± 0.09	0.07	**11**	1.05 ± 0.10	0.75
6	0.64 ± 0.05	0.07	**12**	0.61 ± 0.04	0.03
PAβN	1.17 ± 0.03	0.28	**CCCP**	2.35 ± 0.13	1×10^{-04}

[a]The inhibitory activity was calculated as the fluorescence level of the cells with EPI compounds divided by that of the EPI-free cells at the steady state (24 min for all compounds except **6** and **12**). Values over 1 suggest that the compounds promoted the accumulation of Hoechst by efflux inhibition. **P* value: Student *t*-test was used to calculate the significance, between the cells with and without EPIs. The results were calculated from nine measurements from three independent biological replicates.

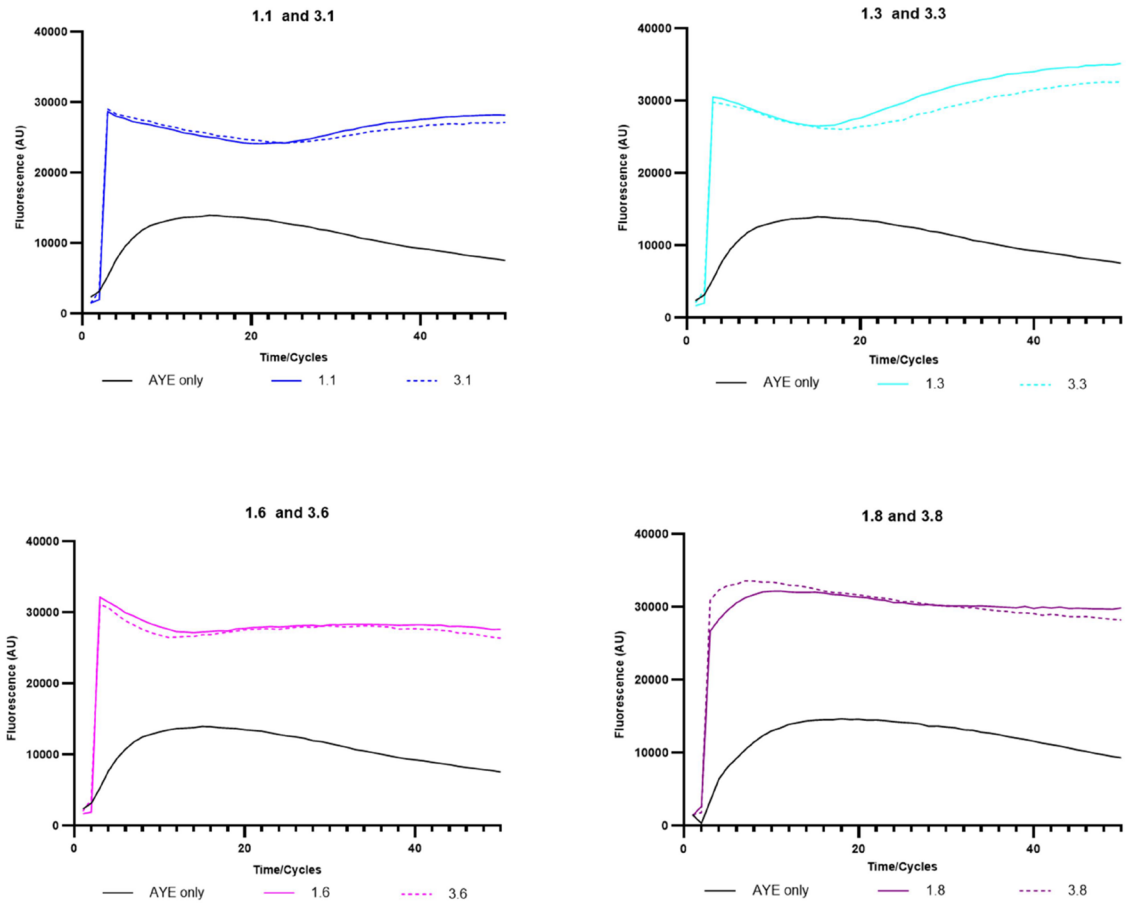

Figure 3. Hoechst accumulation in AYE cells with the addition of some of the most active second-generation quinoline EPI compounds. All results were performed in triplicate, and the curve presented is the fluorescence value of three biological repeats after being blanked against cell free PBSM +G with HOECHST DYE; for clarity, error bars are not shown on the graph, but the SD is included in the end-point measurements shown in Table 2.

inhibitors of AdeABC in *A. baumannii* AYE.[18,22] Potentiation of further antibiotics, rifampicin, clarithromycin, and colistin, were tested in strain AYE (Table S7). Compounds **1, 3, 4** and CCCP decreased the MIC of colistin by more than four-fold. There was no evidence of an increase in colistin MIC with either AdeABC or AdeFGH overexpression. It is possible that the observed potentiation of colistin relates to the PMF uncoupling mechanism of CCCP and this may not be linked to efflux directly, with the EPIs also potentially affecting other cellular functions. Compounds **1** and **4** also showed between 4 and 8-fold potentiation of rifampicin MIC, which was similar to the observed effect of CCCP but much lower potentiation than that observed with PAβN (up to 256-fold potentiation). Clarithromycin was not potentiated by the three quinoline compounds or CCCP, but the MIC was reduced up to 128-fold by PAβN. This data suggests the presence of at least one additional RND-family efflux pump, which is inhibited by PAβN and capable of effluxing rifampicin and clarithromycin, but other efflux pumps/PMF-dependent processes may also affect susceptibility to rifampicin. Since chloramphenicol has been confirmed as a substrate for AdeFGH, and compounds **1**

https://doi.org/10.1021/acsinfecdis.4c00705
ACS Infect. Dis. 2025, 11, 626−638

Table 2. Inhibitory Activity of the Parental Compounds (1 and 3) and the Second-Generation Compounds (25 μg/mL) against Strain AYE as Assessed by Hoechst Accumulation[a]

compound	inhibitory activity	*P* value	compound	inhibitory activity	*P* value
1	1.65 ± 0.10	8.5×10^{-04}	**3**	1.86 ± 0.05	7.83×10^{-06}
1.1	1.11 ± 0.03	0.16	**3.1**	1.06 ± 0.05	0.33
1.2	1.86 ± 0.07	0.0007	**3.2**	2.07 ± 0.04	0.0004
1.3	1.71 ± 0.09	0.0007	**3.3**	1.93 ± 0.14	0.014
1.4	1.93 ± 0.08	0.002	**3.4**	1.82 ± 0.05	6.6×10^{-05}
1.6	2.14 ± 0.04	0.0001	**3.6**	2.11 ± 0.07	0.004
1.7	1.60 ± 0.03	0.0016	**3.7**	1.10 ± 0.06	0.18
1.8	2.22 ± 0.07	0.0012	**3.8**	2.19 ± 0.02	0.001
1.9	1.13 ± 0.07	0.09	**3.9**	1.26 ± 0.03	0.009
1.10	1.20 ± 0.05	0.03	**3.10**	1.06 ± 0.02	0.3
1.11	1.24 ± 0.08	0.023	**3.11**	1.22 ± 0.05	0.025
1.12	1.20 ± 0.002	0.047	**3.12**	1.35 ± 0.02	0.035

[a]The inhibitory activity was calculated as the fluorescence level of the cells added with EPI compounds divided by that of the EPI-free cells at a steady state (after 24 min). *P* value: Student *t*-test was used to calculate the significance, between the cells with and without the EPIs.

Table 3. MICs, Fold-Reduction, and ΣFICi for Chloramphenicol with the Strains Ab5075-UW and Ab5075-CHL Adpated in the Presence of the Second-Generation EPIs[a]

	Ab5075-UW			Ab5075-CHL		
compounds name	MIC (mg/mL)	fold change	ΣFICi	MIC (mg/mL)	fold change	ΣFICi
1	64−128	0−2	0.75−1.25	128	4	1.25
3	64−128	0−2	≤0.625−1.125*	64	8	≤0.25*
1.1	128	0	≤1.25*	128−256	0−2	≤0.5−0.75*
1.2	128	0	≤1.25*	128−256	2−4	≤0.5−0.75*
1.3	32−64	2−4	0.375−0.625	8	64	0.141
1.4	32−64	2−4	0.75−1	64−128	4−8	0.625−0.75
1.5	64	2	1	32−64	8−16	0.56−0.625
1.6	64−128	0−2	0.75−1.25	128−256	2−4	0.5−0.75
1.7	128	0	1.5	128−256	2−4	0.75−1
1.8	64−128	0−2	1−1.5	32	16	0.56
1.9	64	2	≤0.75*	64−128	4−8	≤0.375−0.5*
1.10	64−128	0−2	0.75−1.25	128−256	2−4	0.5−0.75
1.11	32−64	2−4	0.75−1	64−128	4−8	0.625−0.75
1.12	32−64	2−4	0.75−1	64	4	0.625
3.1	64−128	0−2	≤0.75−1.25*	128−256	2−4	≤0.5−0.75*
3.2	64	2	1	64−128	4−8	0.625−0.75
3.3	4−16	8−32	0.56−0.625	8−16	32−64	0.52−0.53
3.4	32−64	2−4	0.75−1	64−128	4−8	0.625−0.75
3.5	64−128	0−2	1.5−2	32	8	1.06
3.6	64	2	1	128	4	0.75
3.7	64−128	0−2	1−1.5	128−256	2−4	0.75−1
3.8	32−64	2−4	0.75−1	16−32	16−32	0.53−0.56
3.9	64	2	≤0.75*	64−128	4−8	≤0.375−0.5*
3.10	64−128	0−2	≤0.625−1.125*	128−256	2−4	≤0.375−0.625*
3.11	16−32	4−8	0.625−0.75	8−16	32−64	0.52−0.53
3.12	32−64	2−4	0.75−1	64−128	4−8	0.625−0.75
CCCP	128	0	2	256	2	1.5
PAβN	64−128	0−2	1.5−2	128−256	2−4	1.25−1.5

[a]For the ΣFICi. * represent the EPI MIC alone is assumed (>200 = 400), so synergy may be higher in these cases.

and **3** showed potentiation of chloramphenicol, these two compounds were selected for further optimization.

Efflux Inhibitory Activity of Second-Generation Quinoline-Type EPI Compounds. The direct antimicrobial activities of the second-generation compounds were measured, and their MIC and optimal testing concentration were determined (Table S5). To allow a systematic evaluation of the efflux pump inhibitory activity between the second-generation compounds and their parent molecules, a single fixed concentration was selected for comparison purposes in the Hoechst assay. A concentration of 25 μg/mL was used as this did not affect growth across the range of compounds tested. Compounds **1.5** and **3.5** were not included in the assay as they produced negative fluorescence levels after normalization, suggesting that they had strong intrinsic fluorescence (results not shown). Most of the 24 s-generation compounds showed strong efflux inhibitory activity in the Hoechst assay (Figures 3 and S4). At the concentration of 25 μg/mL,

https://doi.org/10.1021/acsinfecdis.4c00705
ACS Infect. Dis. 2025, 11, 626−638

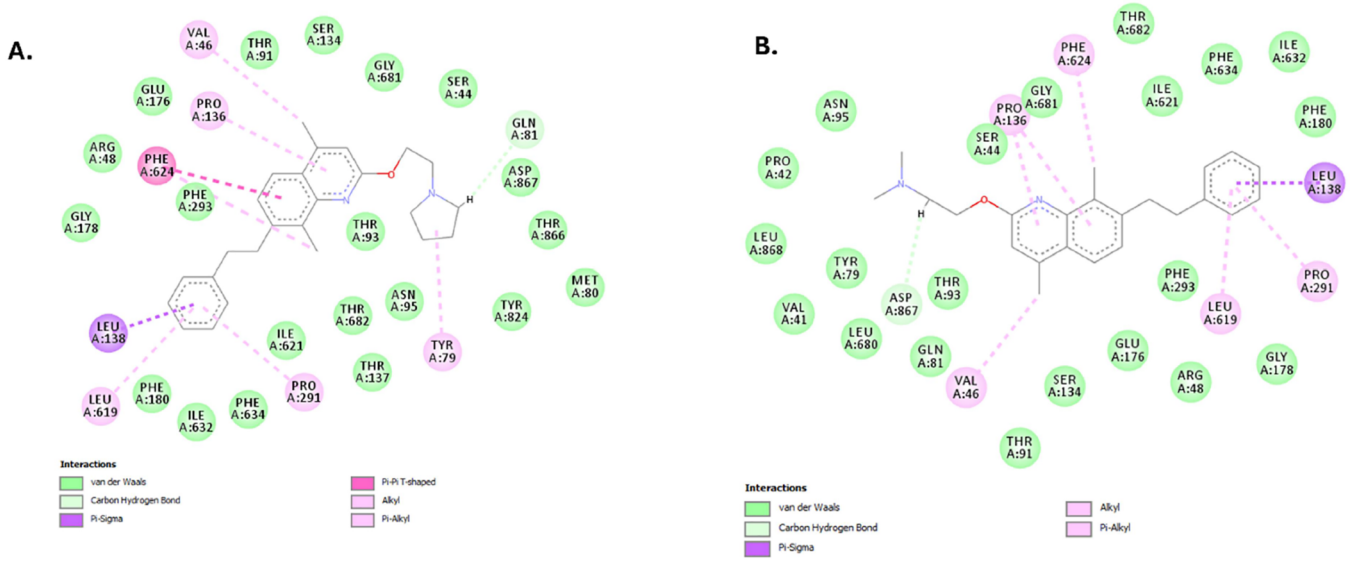

Figure 4. Interactions of **1.3** (A) and **3.3** (B) with the distal binding pocket of AdeG show that the C-7 substituted group interacts with the Phe loop and hydrophobic residues.

compounds **1.6** and **3.6**, which contain a phenyl substitution at the C-7 position, and compounds **1.8** and **3.8**, both containing a quinoline substitution at the C-7 position, showed the best inhibitory activity and an improvement from their parental compounds containing Br at the C-7 position (Table 2). However, the removal of the C-4 and C-8 dimethyl groups led to a reduction of inhibitory activity in each case. For compounds whose optimal testing concentrations are >25 μg/mL, the inhibitory activity was tested again. At a concentration of 100 μg/mL, compounds **1.1**, **3.1**, and **1.7** showed an increase in their inhibitory activity to 1.79, 1.81, and 2.03 (P values are 0.002, 0.002, and 0.001), but compound **3.7** failed to show an improvement.

In terms of the structure−activity relationship (SAR), when the compounds were tested at the same concentration, compound **1** accumulated higher fluorescence than the C-7 thiophene-substituted **1.1** and C-7 pyridyl-substituted **1.9**, and similar fluorescence to the C-7 naphthalene-substituted **1.7**. This trend was consistent with compound **3** analogues, as compound **3** showed better efflux inhibitory activity than compounds **3.1**, **3.7**, and **3.9** (Table 2). Interestingly, the C-7 benzothiophene-substituted compounds **1.2** and **3.2** showed greater efflux inhibitory activities than both compounds **1** and **3**. Among other C-7 substitutions, quinoline (**1.8**/**3.8**) and phenyl (**1.6**/**3.6**) exhibited the highest fluorescence accumulation in AYE cells. Compound **1.8** showed better activity than C-7 naphthalene-substituted **1.7**, suggesting that the nitrogen atom in the quinoline ring of **1.8** played a role in efflux inhibition in the Hoechst assay. However, the C-7 pyridine-substituted compound **1.9** did not show better activity than the C-7 phenyl-substituted compound **1.6**, indicating that either the ring size, the position of the nitrogen atom within the ring, or both are important for efflux inhibition activity in this assay for quinoline-type compounds. While most second-generation compounds had C-7 aromatic or heteroaromatic rings directly connected to the C-7 position of the quinoline ring, a flexible two-carbon linker was introduced in compounds **1.3** and **3.3**, which contained a phenyl substitution at the end of the linker. Both compounds showed good efflux inhibitory activity comparable to that of parent compounds **1** and **3**.

After the test of efflux pump inhibitory activities of the second-generation compounds, the antibiotic potentiation activities of all the compounds were assessed by using gentamicin and chloramphenicol at their test concentrations (Table 3). Two compounds, the flexible C-7 linker containing **3.3** and the C7-phenyl substituted **3.11**, significantly reduced the MIC of chloramphenicol against the wild-type Ab5075-UW by 8−32 and 4−8-fold, respectively. In the AB5075-CHL strain with overexpressed AdeFGH, a much wider range of compounds gave a greater than 4-fold potentiation. Notably, two pairs of compounds, the C-7 flexible linker containing **1.3** (64-fold), and **3.3** (32−64-fold) and the C7-quinoline substituted **1.8** (16-fold), **3.8** (16−32-fold), that showed highest accumulation in Hoechst assay, showed consistently higher chloramphenicol potentiation than their parent compounds, **1** and **3** (4-fold and 8-fold respectively). C-7 phenyl substituted compound **3.11** showed similar levels of chloramphenicol potentiation (32−64-fold) but this was not replicated by the same modification on the compound **1** scaffold (4−8-fold potentiation for **1.11**). It is interesting to note that the fold potentiation of chloramphenicol was achieved with compound **3.3**. and 3.11 in the AB5075-CHL strain (32−64) are higher than the fold increase in MIC between AB5075 and AB5075-CHL (4−8-fold). This would be consistent with the AdeFGH efflux pump having a constitutive level of expression that already impacts the MIC of chloramphenicol in the parental strain, as shown by the potentiation observed by these compounds in AB5075. None of the compounds reduced the MIC of gentamicin in either strain AYE or Ab5075-UW, suggesting that the structural modifications had selectively improved inhibitory activity against AdeFGH and had no notable effect on the inhibition of AdeABC.

As the interaction of the second-generation compounds with the hydrophobic distal binding pocket of AdeG was considered during the design stage, compounds **1.3** and **3.3**, which showed both strong efflux inhibitory activity in the Hoechst accumulation assay and excellent potentiation of chloramphenicol, were selected for further molecular modeling to study their interactions with the distal binding pocket of AdeG. The

https://doi.org/10.1021/acsinfecdis.4c00705
ACS Infect. Dis. 2025, 11, 626−638

flexible C-7 side chain of both compounds effectively interacted with the Phe loop of AdeG, with additional interactions observed with the hydrophobic isoleucine and leucine residues within the binding pocket (Figure 4). The results reinforce the importance of efflux pump inhibitors interacting with the hydrophobic Phe loop within the distal binding pocket of the RND-type efflux pumps.

To further evaluate the mechanism of inhibition by C7-substituted quinolines, we performed docking of the AdeG substrate, chloramphenicol, which was potentiated by the EPIs, to the AdeG efflux pump. Interestingly, chloramphenicol docked at the distal binding site adjacent to the EPIs, with some residues being common between chloramphenicol and the EPIs (Figure S5). This suggests that the C7-substituted quinolines likely act as competitive inhibitors, preventing the efflux of the antibiotic due to steric hindrance.

One of the key observations from the study is the discrepancy between the results obtained from the Hoechst accumulation assay and the antibiotic potentiation assay. The difference in the results between this assay and the antibiotic potentiation assay suggests that the quinoline compounds may inhibit other efflux pumps besides AdeFGH. This indicates that the reduced efflux of Hoechst dyes observed in the assay may not solely be due to the inhibition of AdeFGH but rather a combination of the inhibition of multiple efflux pumps present in the bacterial strains used. Additionally, the Hoechst assay is also a much more sensitive measurement of efflux than the MIC, which is a blunt measurement that is influenced by various factors.

Despite the limitations of the Hoechst accumulation assay as a direct measure of AdeFGH inhibition, the data indicate that eight pairs of compounds with specific modifications to the quinoline core scaffold showed selective potentiation of the AdeFGH substrate antibiotic chloramphenicol. Notably, these compounds did not show a similar potentiation effect on the AdeABC substrate antibiotic gentamicin. This selective potentiation underscores the specificity of these quinoline-based efflux pump inhibitors (EPIs) toward AdeFGH, suggesting that the quinoline-based compounds reported in this study inhibit the AdeFGH pump strongly enough to result in significant potentiation of its antibiotic substrate.

Furthermore, structural analysis revealed that some second-generation compounds exhibited strong efflux pump inhibitory activity in both the Hoechst accumulation assay and the antibiotic potentiation assay. Specifically, compounds **1.8** and **3.8** demonstrated the best efflux pump inhibitory activity, correlating with their structural features. These compounds possessed a heterononaromatic group (either pyrrolidine or dimethyl amine) and a quinoline moiety at the C-2 and C-7 positions of the core quinoline ring, along with C-4 and C-8 methyl groups. This structure−activity relationship information suggests that it is feasible to develop selective inhibitors of RND efflux pumps using quinoline as a core scaffold that could potentiate clinically used antibiotics that are substrates of these efflux pumps.

Finally, the toxicity of the most active compounds was tested using the *Galleria mellonella* nonanimal toxicity assay. None of the compounds showed any notable toxicity at the 20 mg/kg dose level, suggesting that this quinoline scaffold is nontoxic at the doses studied (Figure S6). The ability of these compounds to selectively potentiate the activity of chloramphenicol, coupled with their low toxicity, supports their potential as therapeutic agents. Further optimization and structural refinement of these compounds could lead to the development of clinically useful efflux pump inhibitors that could be coadministered with antibiotics to combat bacterial resistance.

CONCLUSIONS

Quinoline-type compounds were developed in this study and assessed as EPIs for *A. baumannii* AdeABC, AdeFGH, and AdeIJK. Data suggested that the compounds could inhibit efflux from AdeFGH but not the closely related pump AdeABC, potentially due to specific interactions with Phe residues within the binding interface. The study allowed us to look at both general factors affecting dye accumulation such as efflux inhibition, especially in isogenic lines with mutations in key regulators or efflux pumps, and the function of specific pumps. Although chloramphenicol has been reported as a substrate for AdeIJK, non-RND efflux systems like AbeM and AbeS,[24−26] and a novel permease-based efflux system (Ab5075-UW[27]), there was a clear MIC phenotype in this study, which could be linked to a mutation in AdeL. Previous studies have defined a similar phenotype associated with gentamicin resistance in AYE and AB5075.[18]

Although the study did not produce an efflux pump inhibitor capable of potentiation activity of clinically useful antibiotics to below the resistance breakpoint, it did provide valuable information on the inhibitor specificity of different but structurally related pumps. This may enable the future development of EPIs with a broader spectrum of activity against RND-family efflux pumps. The variability in the level of potentiation observed for different compounds suggests that these compounds, in addition to considering them for further med-chem modification to obtain potential development candidates, can be used as probes for efflux pump SAR studies.

MATERIALS AND METHODS

Chemistry. The solvent and reagents used for the synthesis were purchased from various commercial sources, including Sigma-Aldrich, Fisher Scientific, and Fluorochem. ^{1}H and ^{13}C nuclei nuclear magnetic resonance (NMR) analyses were performed on a Spectrospin 400 MHz spectrometer (from Bruker) by using deuterated solvents for the preparation of the samples. The spectra of each compound were analyzed using Topspin 3.5pl7 software (Bruker). The chemical shifts were reported relative to trimethylsilane (TMS) used as standard (0.00 ppm). Signals were identified and described as singlet (s), doublet (d), t (triplet), or m (multiplets). Coupling constants were shown in Hertz (Hz). High-resolution mass spectrometry (HRMS) was carried out on an Exactive HCD Orbitrap mass spectrometer (Thermo Scientific). LC-MS analyses were performed on a Waters Alliance 2695 system, eluting in a gradient with a flow rate of 0.5 mL/min using a solvent gradient starting with 5% acetonitrile that was increased to 95% acetonitrile over a 7.5 min time period (ESI). The analyses were performed on a Monolithic C18 50 × 4.60 mm column (made by Phenomenex). UV detection was performed on a Diode Array Detector. Mass spectra were registered in both the ESI+ and ESI- modes. The synthesis and characterization of the quinoline-based EPIs reported in this paper can be found in the Supporting Information.

Bacterial Strains and Culture Conditions. All strains (Table S1) were grown in tryptic soy broth (TSB) (SIGMA) or on tryptic soy agar (TSA) (Biomerieux) at 37 °C unless otherwise stated. All of the chemicals used in this study were

https://doi.org/10.1021/acsinfecdis.4c00705
ACS Infect. Dis. 2025, 11, 626−638

purchased from Sigma unless otherwise stated. All antibiotic stock solutions were dissolved in water to the stock concentration except for chloramphenicol (100% ethanol) and ciprofloxacin (diluted acetic acid). Upon use, they were diluted to the desired concentration in TSB. All quinoline-based compounds tested in this study were dissolved in DMSO at a concentration of 10 mg/mL to make the stock solution, and they were diluted to the desired concentration in TSB before use in the test. CCCP and PAβN stock solutions were made in DMSO and dH_2O, respectively, and diluted in TSB.

Minimum Inhibitory Concentration (MIC) Test. A broth-microdilution method was used in accordance with the methodology laid out by the European Committee on Antimicrobial Susceptibility Testing (EUCAST) with modifications, as described previously. All MICs were performed in TSB media using polystyrene 96-well plates (Corning, Flintshire UK) except for colistin, where polypropylene plates (Greiner Bio-One Ltd., Stonehouse UK) and noncation adjusted Mueller Hinton media were used. Bacteria were grown in media overnight at 37 °C, 200 rpm. They were then diluted to a concentration of 1×10^6 CFU/mL (OD_{600} = 0.01) and antibiotics were added as a two-fold dilution series, either alone or in combination with potential EPIs. The plate was then incubated at 37 °C statically for 20 h after which the absorbance at 600 nm was read. After background subtraction, the lowest concentration of antibiotic where the OD_{600} value was below 0.1 was considered as the MIC value. All results were carried out at least in triplicates. Bacterial growth in the presence of compounds was monitored by taking an OD_{600} reading every hour for 20 h using a FLUOstar Omega plate reader (BMG Labtech GmbH, Ortenberg, Germany).

Hoechst Assay. The Hoechst dye (H33342 bisbenzimide) accumulation assay to measure efflux in *A. baumannii* strains, was carried out as described previously with the following modifications.[23] Compounds to be tested were diluted in DMSO to a concentration 25 times that of the test concentration. Bacteria were grown in TSB media overnight at 37 °C, 200 rpm. 250 μL of the overnight culture was added to 5 mL of fresh TSB media, which was then further incubated at 37 °C, 200 rpm until the OD_{600} reached 0.4−0.6. Bacterial cells were harvested by centrifugation at 4500 g for 10 min at room temperature. The supernatant was discarded, and the cell pellet was resuspended in PBSM+G (PBS buffer with 20 mM glucose and 1 mM $MgSO_4$. The OD_{600} of the cell suspension was measured and adjusted to 0.5. A black bottom 96-well plate (Corning, Flintshire UK) was used in this experiment. In each well, 176 μL of cell suspension, together with 4 μL of compound stock solution and 4 μL of DMSO or 4ul media, were added. The plate was incubated for 15 min at 37 °C in the plate reader before 20 μL of 25 μM HOECHST DYE stock solution in dH2O, was injected into each well except for the blank controls to give a final well volume of 200 μL. The fluorescence level (excitation and emission filter at 355 and 460 nm) was measured every 2.6 min for 133 min after the addition of the HOECHST dyes. Hoechst dye has been found to adsorb on polytetrafluoroethylene-coated material in an aqueous solvent, with a concomitant fluorescence drop later in the Hoechst assay.[28] To mitigate this effect the steady fluorescence level at 24 min after the addition of the Hoechst dye was analyzed, rather than the end point at 133 min. For each compound with each strain, the average value of the three replicate wells was calculated and then corrected against the compound control. Data were analyzed from three independent biological replicates.

Development of the Antibiotic-Resistant Strains. A gradient plate method was used to select resistant *A. baumannii* strains to three different antibiotics (gentamicin, chloramphenicol, ceftazidime).[29], known to be substrates for the three efflux pump systems. To adapt each strain to each antibiotic, 20 mL of molten TSA containing no antibiotic was set in a standard Petri dish, where one side of the plate was elevated 1 cm to allow a slope to form (Figure S1). After the slope had been set, 20 mL of TSA containing antibiotic at a concentration of 4-fold the MIC level was added to the plate and allowed to set. Plates were rested overnight at room temperature to ensure diffusion of the antibiotic. 100 mL of bacterial from overnight culture was inoculated on each plate, and the plates were incubated overnight at 37 °C. Four colonies nearest to the zone of inhibition from each plate were picked and restreaked onto a fresh TSA plate with no antibiotic for storage. From the storage plate, the MIC of individual colonies was tested. The whole procedure was repeated at a higher concentration across the gradient until a significant increase of MIC (≥4-fold) was obtained. Clones of interest were sent for whole genome sequencing to identify arising mutations.

Whole Genome Sequencing and Analysis. Bacterial DNA of both wildtype and mutants was purified with a Wizard genomic DNA purification kit (Promega, Wisconsin, US). DNA was then tagged and multiplexed with the Nextera XT DNA kit (Illumina, San Diego, US) and sequenced by Public Health England Genomic Services and Development Unit, (PHE-GSDU) on an Illumina (HiSeq 2500) with paired-end read lengths of 150 bp. A minimum of 150 Mb of Q30 quality data were obtained for each isolate. FastQ files were trimmed to a quality using Trimmomatic. SPAdes 3.1.1 was used to produce draft chromosomal assemblies, and contigs of less than 1 kb were filtered out.[30] FastQ reads from selected isolates were mapped to their respective parental strain pre-exposure chromosomal sequence using BWA 0.7.5.[31] Bam format files were generated using Samtools,[32] and VCF files were constructed using the GATK2 Unified Genotyper (version 0.0.7).[33] They were further filtered using the following filtering criteria to identify high-confidence SNPs: mapping quality > 30; genotype quality > 40; variant ratio > 0.9; read depth > 10. All the above-described sequencing analyses were performed using PHE Galaxy.[34] BAM files were visualized in Integrative Genomics Viewer (IGV) version 2.3.55.[35] Whole genome alignment and phylogenetic tree generation were performed using progressive alignment in Mauve Version 20150226 build 10. Tree visualization was performed in FigTree Version 1.4.3.

Q-PCR Method and Primers for Checking the Overexpression of Pump Genes. Real-time PCR (RT-PCR) was used to measure the expression of *adeB, adeR, adeS, adeG, adeL, adeJ,* and *adeN* in the Ab5075 transposon mutants, chloramphenicol adapted and Ab5075-UW W/T strains. The method was adapted from *Wand et al.*[20] The primers used for each gene are listed in Table S8. The primer efficiency was first checked. In the test, 50 μL of PCR reaction, containing 1 μL of template DNA; 0.5 μL of each primer, 25 μL of GoTaq reaction buffer, and 23 μL of dH_2O were set up. After obtaining the PCR products, they were diluted to 10^{-2}, 10^{-4}, 10^{-5}, 10^{-6}, 10^{-7}, 10^{-8}, 10^{-9}, 10^{-10}, and 10^{-11}. For each set of primers, 7 dilution products from 10^{-5} to 10^{-11} were used in

https://doi.org/10.1021/acsinfecdis.4c00705
ACS Infect. Dis. 2025, 11, 626−638

the efficiency check test. Seven reactions of 20 μL mixture, each containing 10 μL of SYBR green master mix, 0.2 μL of each 10 mM primer stock, 6 μL of PCR product dilution, and 3.6 μL of dH_2O, were set up. For each set of primers, 1 no-template control was involved, in which 6 μL of diluted PCR product was replaced with 6 μL of dH_2O. Each reaction mixture was loaded into a 96-multiwell PCR plate (SIGMA) before amplifying using the StepOnePlus real-time PCR system.

After the primer efficiency was checked, the RT-PCR of each gene was carried out. Bacterial overnight cultures were diluted in TSB to an OD_{600} of 0.1, and further incubated until reaching the mid-log phase (OD_{600} = 0.5) and cells were then harvested by using the RNA protect bacteria reagent (Qiagen). Afterward, the RNA of each bacterial strain was extracted by using the RNeasy mini kit (Qiagen), including on-column DNase treatment according to the manufacturer's instructions. Additionally, 5 μg of RNA was treated with a DNA-free kit (Ambion), of which 0.2 μg of RNA was reverse transcribed by using the SuperScript III first-strand synthesis system for RT-PCR (Invitrogen) according to the manufacturer's instructions. qPCR was then repeated at least three times on each sample using a StepOnePlus real-time PCR system and Fast SYBR green master mix (Life Technologies). After the RT-PCR was finished, data were analyzed with the Expression Suite Software version 1.0.3 (Life Technologies) by using the *recN, proC,* and *fabD* as endogenous controls and taking primer efficiency into account.

Molecular Docking. Since the structures of the AdeB and AdeG have not been validated, the molecular modeling work was based on the models of AcrB and MexB, respectively. First, the amino acid sequences of AdeB (B7I7F7), AcrB (P31224), AdeG (A0A090C131) and MexB (P52002) were downloaded from Uniprot. AdeB and AcrB, were 50.36% identical while AdeG and MexB were 41.97%. The crystal structures of efflux pump AcrB (1IWG) and MexB (3W9J) were downloaded from the Protein Data Bank (http://www.rcsb.org/) and used as the basis for homology modeling of AdeB and AdeG using Swiss-model.[36] Any missing parts of the predicted AdeB and AdeG structure were amended by using the Biovia Discovery studio visualizer.[37] Finally, the program Amber was used to minimize the energy of the structures.[38,39] AutoDock SMINA,[40] which fuses the AutoDock Vina scoring function by default, was first applied for the blind molecular docking of potential EPI compounds to each structure. This identified the best binding site in the target by exploring all of the possible binding cavities of the transporter. SMINA was performed with default settings, which sampled nine ligand conformations using the Vina docking routine of stochastic sampling. Afterward, GOLD molecular docking was used to dock the compounds to the best binding site located by SMINA of the efflux pump for performing flexible molecular docking.[41] Based on the fitness function scores and ligand binding positions, the ten best-docked poses for the compounds were selected. Among the ten poses, the higher fitness function score of poses, generated using the GOLD program that has the more negative GOLD fitness energy value, reveals the best-docked pose for each compound. For structural optimization of the docked ligand-protein complexes, the docked complexes were imported in PDB format in the YASARA structure, and all residues that were in contact with the ligand were made flexible. This was followed by energy minimization of the complex and structure optimization using the semiempirical quantum mechanics (MOPAC) command.

***Galleria mellonella* Survival Test.** Wax moth larvae (*Galleria mellonella*) were kept on wood chips at 14 °C in the dark until use. For experiments, it was assumed that each *Galleria* had a hemolymph volume of 50 μL and could tolerate 10 μL of liquid injection. Therefore, the stock solution of each compound was prepared at 6 times the concentration they were going to be tested. For each compound at each test concentration, 10 μL of compound stock solution was injected into 10 *Galleria* via the foremost probe using a Hamilton syringe. Ten of the control larvae were injected with 10 μL of PSB to control for potential lethal effects from the injection process. After injection, larvae were kept at 37 °C inside the Petri dishes, and the number of live larvae was recorded every 24 h for 5 days. This method was adapted from Wand et al.[42]

■ ASSOCIATED CONTENT

Supporting Information

The Supporting Information is available free of charge at https://pubs.acs.org/doi/10.1021/acsinfecdis.4c00705.

Collection of bacterial strains, gene primers, MIC data, LC-MS method, experimental details for the synthesis of quinoline EPIS, NMR spectra and HRMS, and molecular formula strings (PDF)

■ AUTHOR INFORMATION

Corresponding Authors

J. Mark Sutton − *UK Health Security Agency, Research and Development Institute, National Infection Service, Salisbury, Wiltshire SP4 0JG, U.K.; Institute of Pharmaceutical Science, School of Cancer & Pharmaceutical Sciences, King's College London, London SE1 9NH, U.K.*; Phone: +44 (0) 1980 612649; Email: mark.sutton@phe.gov.uk

Khondaker Miraz Rahman − *Institute of Pharmaceutical Science, School of Cancer & Pharmaceutical Sciences, King's College London, London SE1 9NH, U.K.*; orcid.org/0000-0001-8566-8648; Phone: +44 (0) 2078 481891; Email: k.miraz.rahman@kcl.ac.uk

Authors

Yiling Zhu − *UK Health Security Agency, Research and Development Institute, National Infection Service, Salisbury, Wiltshire SP4 0JG, U.K.; Institute of Pharmaceutical Science, School of Cancer & Pharmaceutical Sciences, King's College London, London SE1 9NH, U.K.*

Charlotte K. Hind − *UK Health Security Agency, Research and Development Institute, National Infection Service, Salisbury, Wiltshire SP4 0JG, U.K.*; orcid.org/0000-0002-3763-3106

Taha Al-Adhami − *Institute of Pharmaceutical Science, School of Cancer & Pharmaceutical Sciences, King's College London, London SE1 9NH, U.K.*

Matthew E. Wand − *UK Health Security Agency, Research and Development Institute, National Infection Service, Salisbury, Wiltshire SP4 0JG, U.K.*

Melanie Clifford − *UK Health Security Agency, Research and Development Institute, National Infection Service, Salisbury, Wiltshire SP4 0JG, U.K.*

Complete contact information is available at: https://pubs.acs.org/10.1021/acsinfecdis.4c00705

https://doi.org/10.1021/acsinfecdis.4c00705
ACS Infect. Dis. 2025, 11, 626−638

Author Contributions

Y.Z., C.K.H., M.C., and K.M.R. carried out experiments, Y.Z., T.A-.A., M.E.W., and K.M.R. analyzed data, C.K.H., J.M.S., and K.M.R. supervised the experiments, Y.Z. and K.M.R. wrote the manuscript, All authors contributed to the edit and review of the manuscript. All authors agreed to the final version of the manuscript.

Notes

The authors declare no competing financial interest.

■ ACKNOWLEDGMENTS

This work was supported by an Industrial PhD award for Yiling Zhu (Project ID 537242), a research grant from the Medical Research Council (MR/W018594/1), and through the UKHSA Grant in Aid Project 109502 and 109505. We also gratefully acknowledge the provision of transposon library strains, as described in Gallagher *et al* 2015 from the Manoil lab.[43]

■ REFERENCES

(1) WHO. *WHO Bacterial Priority Pathogens List, 2024: Bacterial Pathogens of Public Health Importance to Guide Research, Development and Strategies to Prevent and Control Antimicrobial Resistance*; 2024. Available from: https://iris.who.int/bitstream/handle/10665/376776/9789240093461-eng.pdf?sequence=1.

(2) Lewis, K. Platforms for Antibiotic Discovery. *Nat. Rev. Drug Discovery* **2013**, *12* (5), 371−387.

(3) Coyne, S.; Courvalin, P.; Périchon, B. Efflux-Mediated Antibiotic Resistance in *Acinetobacter* spp. *Antimicrob. Agents Chemother.* **2011**, *55* (3), 947−953.

(4) Putman, M.; van Veen, H. W.; Konings, W. N. Molecular Properties of Bacterial Multidrug Transporters. *Microbiol. Mol. Biol. Rev.* **2000**, *64* (4), 672−693.

(5) Marchand, I.; Damier-Piolle, L.; Courvalin, P.; Lambert, T. Expression of the RND-Type Efflux Pump AdeABC in *Acinetobacter baumannii* Is Regulated by the AdeRS Two-Component System. *Antimicrob. Agents Chemother.* **2004**, *48* (9), 3298−3304.

(6) Magnet, S.; Courvalin, P.; Lambert, T. Resistance-Nodulation-Cell Division-Type Efflux Pump Involved in Aminoglycoside Resistance in *Acinetobacter baumannii* Strain BM4454. *Antimicrob. Agents Chemother.* **2001**, *45* (12), 3375−3380.

(7) Rodríguez-Baño, J.; Marti, S.; Soto, S.; Fernández-Cuenca, F.; Cisneros, J. M.; Pachón, J.; Pascual, A.; Martínez-Martínez, L.; McQueary, C.; Actis, L. A.; Vila, J. Biofilm Formation in *Acinetobacter baumannii*: Associated Features and Clinical Implications. *Clin. Microbiol. Infect.* **2008**, *14* (3), 276−278.

(8) Rosenfeld, N.; Bouchier, C.; Courvalin, P.; Périchon, B. Expression of the Resistance-Nodulation-Cell Division Pump AdeIJK in *Acinetobacter baumannii* Is Regulated by AdeN, a TetR-Type Regulator. *Antimicrob. Agents Chemother.* **2012**, *56* (5), 2504−2510.

(9) Coyne, S.; Rosenfeld, N.; Lambert, T.; Courvalin, P.; Périchon, B. Overexpression of Resistance-Nodulation-Cell Division Pump AdeFGH Confers Multidrug Resistance in *Acinetobacter baumannii*. *Antimicrob. Agents Chemother.* **2010**, *54* (10), 4389−4393.

(10) He, X.; Lu, F.; Yuan, F.; Jiang, D.; Zhao, P.; Zhu, J.; Cheng, H.; Cao, J.; Lu, G. Biofilm Formation Caused by Clinical *Acinetobacter baumannii* Is Associated with Overexpression of the AdeFGH Efflux Pump. *Antimicrob. Agents Chemother.* **2015**, *59* (8), 4817−4825.

(11) Fernando, D.; Zhanel, G.; Kumar, A. Antibiotic Resistance and Expression of Resistance-Nodulation-Division Pump- and Outer Membrane Porin-Encoding Genes in *Acinetobacter* Species Isolated from Canadian Hospitals. *Can. J. Infect. Dis. Med. Microbiol.* **2013**, *24* (1), 17−21.

(12) Lomovskaya, O.; Watkins, W. Inhibition of Efflux Pumps as a Novel Approach to Combat Drug Resistance in Bacteria. *J. Mol. Microbiol. Biotechnol.* **2001**, *3* (2), 225−236.

(13) Lomovskaya, O.; Warren, M. S.; Lee, A.; Galazzo, J.; Fronko, R.; Lee, M.; Blais, J.; Cho, D.; Chamberland, S.; Renau, T.; Leger, R.; Hecker, S.; Watkins, W.; Hoshino, K.; Ishida, H.; Lee, V. J. Identification and Characterization of Inhibitors of Multidrug Resistance Efflux Pumps in *Pseudomonas aeruginosa*: Novel Agents for Combination Therapy. *Antimicrob. Agents Chemother.* **2001**, *45* (1), 105−116.

(14) Cortez-Cordova, J.; Kumar, A. Activity of the Efflux Pump Inhibitor Phenylalanine-Arginine Beta-Naphthylamide Against the AdeFGH Pump of *Acinetobacter baumannii*. *Int. J. Antimicrob. Agents* **2011**, *37* (5), 420−424.

(15) Tambat, R.; Kinthada, R. K.; Sariyer, A. S.; Leus i, V.; Sariyer, E.; D'Cunha, N.; Zhou, H.; Leask, M.; Walker, J. K.; Zgurskaya, H. I. AdeIJK Pump-Specific Inhibitors Effective Against Multidrug Resistant *Acinetobacter baumannii*. *ACS Infect. Dis.* **2024**, *10* (6), 2239−2249.

(16) Ghisalberti, D.; Mahamoud, A.; Chevalier, J.; Baitiche, M.; Martino, M.; Pagès, J. M.; Barbe, J. Chloroquinolines Block Antibiotic Efflux Pumps in Antibiotic-Resistant *Enterobacter aerogenes* Isolates. *Int. J. Antimicrob. Agents* **2006**, *27* (6), 565−569.

(17) Chiu, C. H.; Lee, H. Y.; Tseng, L. Y.; Chen, C. L.; Chia, J. H.; Su, L. H.; Liu, S. Y. Mechanisms of Resistance to Ciprofloxacin, Ampicillin/Sulbactam, and Imipenem in *Acinetobacter baumannii* Clinical Isolates in Taiwan. *Int. J. Antimicrob. Agents* **2010**, *35* (4), 382−386.

(18) Richmond, G. E.; Evans, L. P.; Anderson, M. J.; Wand, M. E.; Bonney, L. C.; Ivens, A.; Chua, K. L.; Webber, M. A.; Sutton, J. M.; Peterson, M. L.; Piddock, L. J. The *Acinetobacter baumannii* Two-Component System AdeRS Regulates Genes Required for Multidrug Efflux, Biofilm Formation, and Virulence in a Strain-Specific Manner. *mBio* **2016**, *7* (2), No. e00430-16.

(19) Wand, M. E.; Jamshidi, S.; Bock, L. J.; Rahman, K. M.; Sutton, J. M. SmvA is an Important Efflux Pump for Cationic Biocides in *Klebsiella pneumoniae* and Other *Enterobacteriaceae*. *Sci. Rep.* **2019**, *9* (1), 1344.

(20) Wand, M. E.; Bock, L. J.; Bonney, L. C.; Sutton, J. M. Mechanisms of Increased Resistance to Chlorhexidine and Cross-Resistance to Colistin Following Exposure of *Klebsiella pneumoniae* Clinical Isolates to Chlorhexidine. *Antimicrob. Agents Chemother.* **2017**, *61* (1), No. e01162-16.

(21) Coyne, S.; Guigon, G.; Courvalin, P.; Périchon, B. Screening and Quantification of the Expression of Antibiotic Resistance Genes in *Acinetobacter baumannii* with a Microarray. *Antimicrob. Agents Chemother.* **2010**, *54* (1), 333−340.

(22) Jamshidi, S.; Sutton, J. M.; Rahman, K. M. Computational Study Reveals the Molecular Mechanism of the Interaction Between the Efflux Inhibitor PAβN and the AdeB Transporter from *Acinetobacter baumannii*. *ACS Omega* **2017**, *2* (6), 3002−3016.

(23) Richmond, G. E.; Chua, K. L.; Piddock, L. J. V. Efflux in *Acinetobacter baumannii* Can Be Determined by Measuring Accumulation of H33342 (Bis-Benzamide). *J. Antimicrob. Chemother.* **2013**, *68* (7), 1594−1600.

(24) Damier-Piolle, L.; Magnet, S.; Brémont, S.; Lambert, T.; Courvalin, P. AdeIJK, a Resistance-Nodulation-Cell Division Pump Effluxing Multiple Antibiotics in *Acinetobacter baumannii*. *Antimicrob. Agents Chemother.* **2008**, *52* (2), 557−562.

(25) Su, X. Z.; Chen, J.; Mizushima, T.; Kuroda, T.; Tsuchiya, T. AbeM, an H+-Coupled *Acinetobacter baumannii* Multidrug Efflux Pump Belonging to the MATE Family of Transporters. *Antimicrob. Agents Chemother.* **2005**, *49* (10), 4362−4364.

(26) Srinivasan, V. B.; Rajamohan, G.; Gebreyes, W. A. Role of AbeS, a Novel Efflux Pump of the SMR Family of Transporters, in Resistance to Antimicrobial Agents in *Acinetobacter baumannii*. *Antimicrob. Agents Chemother.* **2009**, *53* (12), 5312−5316.

(27) Karalewitz, A. P. A.; Miller, S. I. Multidrug-Resistant *Acinetobacter baumannii* Chloramphenicol Resistance Requires an Inner Membrane Permease. *Antimicrob. Agents Chemother.* **2018**, *62* (8), No. e00113-18.

https://doi.org/10.1021/acsinfecdis.4c00705
ACS Infect. Dis. 2025, 11, 626−638

(28) Verchere, A.; Broutin, I.; Picard, M. Hoechst Likes to Play Hide and Seek··· Use It with Caution! *Anal. Biochem.* **2013**, *440* (2), 117−119.
(29) Maeder, M. L.; Thibodeau-Beganny, S.; Sander, J. D.; Voytas, D. F.; Joung, J. K. Oligomerized Pool Engineering (OPEN): An ″Open-Source″ Protocol for Making Customized Zinc-Finger Arrays. *Nat. Protoc.* **2009**, *4* (10), 1471−1501.
(30) Bankevich, A.; Nurk, S.; Antipov, D.; Gurevich, A. A.; Dvorkin, M.; Kulikov, A. S.; Lesin, V. M.; Nikolenko, S. I.; Pham, S.; Prjibelski, A. D.; Pyshkin, A. V.; Sirotkin, A. V.; Vyahhi, N.; Tesler, G.; Alekseyev, M. A.; Pevzner, P. A. A New Genome Assembly Algorithm and Its Applications to Single-Cell Sequencing. *J. Comput. Biol.* **2012**, *19* (5), 455−477.
(31) Li, H.; Durbin, R. Fast and Accurate Short Read Alignment with Burrows−Wheeler Transform. *Bioinformatics* **2009**, *25* (14), 1754−1760.
(32) Li, H.; Handsaker, B.; Wysoker, A.; Fennell, T.; Ruan, J.; Homer, N.; Marth, G.; Abecasis, G.; Durbin, R. The Sequence Alignment/Map Format and SAMtools. *Bioinformatics* **2009**, *25* (16), 2078−2079.
(33) McKenna, A.; Hanna, M.; Banks, E.; Sivachenko, A.; Cibulskis, K.; Kernytsky, A.; Garimella, K.; Altshuler, D.; Gabriel, S.; Daly, M.; DePristo, M. A. The Genome Analysis Toolkit: A MapReduce Framework for Analyzing Next-Generation DNA Sequencing Data. *Genome Res.* **2010**, *20* (9), 1297−1303.
(34) Afgan, E.; Baker, D.; van den Beek, M.; Blankenberg, D.; Bouvier, D.; Čech, M.; Chilton, J.; Clements, D.; Coraor, N.; Eberhard, C.; Grüning, B.; Guerler, A.; Hillman-Jackson, J.; Von Kuster, G.; Rasche, E.; Soranzo, N.; Turaga, N.; Taylor, J.; Nekrutenko, A.; Goecks, J. The Galaxy Platform for Accessible, Reproducible, and Collaborative Biomedical Analyses: 2016 Update. *Nucleic Acids Res.* **2016**, *44* (W1), W3−W10.
(35) Robinson, J. T.; Thorvaldsdóttir, H.; Winckler, W.; Guttman, M.; Lander, E. S.; Getz, G.; Mesirov, J. P. Integrative Genomics Viewer. *Nat. Biotechnol.* **2011**, *29* (1), 24−26.
(36) Waterhouse, A.; Bertoni, M.; Bienert, S.; Studer, G.; Tauriello, G.; Gumienny, R.; Heer, F. T.; de Beer, T. A. P.; Rempfer, C.; Bordoli, L.; Lepore, R.; Schwede, T. SWISS-MODEL: Homology Modelling of Protein Structures and Complexes. *Nucleic Acids Res.* **2018**, *46*, 296−303.
(37) Biovia, D. S. *Discovery Studio Modeling Environment*; Dassault Systèmes: San Diego, 2017.
(38) Case, D. A.; Darden, T. A.; Cheatham, T. E.; Simmerling, III, C. L.; Wang, J; Duke, R. E.; Luo, R.; Walker, R. C.; Zhang, W.; Merz, K. M.; Roberts, B.; Hayik, S.; Roitberg, A.; Seabra, G.; Swails, J.; Götz, A. W.; Kolossváry, I.; Wong, K. F.; Paesani, F.; Vanicek, J.; Wolf, R. M.; Liu, J.; Wu, X.; Brozell, S. R.; Steinbrecher, T.; Gohlke, H.; Cai, Q.; Ye, X.; Wang, J.; Hsieh, M.-J.; Cui, G.; Roe, D. R.; Mathews, D. H.; Seetin, M. G.; Salomon-Ferrer, R.; Sagui, C.; Babin, V.; Luchko, T.; Gusarov, S.; Kovalenko, A.; Kollman, P. A. *AMBER 12*; University of California: San Francisco, 2012.
(39) Case, D. A.; Cheatham, T. E., III; Darden, T.; Gohlke, H.; Luo, R.; Merz, K. M.; Onufriev, A.; Simmerling, C.; Wang, B.; Woods, R. The Amber Biomolecular Simulation Programs. *J. Comput. Chem.* **2005**, *26*, 1668−1688.
(40) Koes, D. R.; Baumgartner, M. P.; Camacho, C. J. Lessons Learned in Empirical Scoring with Smina from the CSAR 2011 Benchmarking Exercise. *J. Chem. Inf. Model.* **2013**, *53*, 1893−1904.
(41) Jones, G.; Willett, P.; Glen, R. C.; Leach, A. R.; Taylor, R. Development and Validation of a Genetic Algorithm for Flexible Docking. *J. Mol. Biol.* **1997**, *267*, 727−748.
(42) Wand, M. E.; Müller, C. M.; Titball, R. W.; Michell, S. L. Macrophage and *Galleria mellonella* Infection Models Reflect the Virulence of Naturally Occurring Isolates of *Burkholderia pseudomallei*, *B. thailandensis*, and *B. oklahomensis*. *BMC Microbiol.* **2011**, *11*, 11.
(43) Gallagher, L. A.; Ramage, E.; Weiss, E. J.; Radey, M.; Hayden, H. S.; Held, K. G.; Huse, H. K.; Zurawski, D. V.; Brittnacher, M. J.; Manoil, C. Resources for Genetic and Genomic Analysis of Emerging Pathogen *Acinetobacter baumannii*. *J. Bacteriol.* **2015**, *197* (12), 2027−2035.

https://doi.org/10.1021/acsinfecdis.4c00705
ACS Infect. Dis. 2025, 11, 626−638